Mario Kleo, Holger Mößinger, Florentine Förster-Zügel, Helmut F. Schlaak, Thomas Wallmersperger

Investigation of the thermal effects in dynamically driven dielectric elastomer actuators

Erstveröffentlichung in / First published in:

SPIE Smart Structures and Materials + Nondestructive Evaluation and Health Monitoring. Denver, 2018. Bellingham: SPIE, Vol. 10594 *[Zugriff am: 02.05.2019]*.

DOI: https://doi.org/10.1117/12.2295924

Investigation of the thermal effects in dynamically driven dielectric elastomer actuators

Mario Kleo, Holger Mößinger, Florentine Förster-Zügel, Helmut F. Schlaak, Thomas Wallmersperger

Mario Kleo, Holger Mößinger, Florentine Förster-Zügel, Helmut F. Schlaak, Thomas Wallmersperger, "Investigation of the thermal effects in dynamically driven dielectric elastomer actuators," Proc. SPIE 10594, Electroactive Polymer Actuators and Devices (EAPAD) XX, 105940G (27 March 2018); doi: 10.1117/12.2295924

SPIE.

Event: SPIE Smart Structures and Materials + Nondestructive Evaluation and Health Monitoring, 2018, Denver, Colorado, United States

Investigation of the thermal effects in dynamically driven dielectric elastomer actuators

Mario Kleo[a], Holger Mößinger[b], Florentine Förster-Zügel[b], Helmut F. Schlaak[b], and Thomas Wallmersperger[a]

[a]Institut für Festkörpermechanik, Technische Universität Dresden, 01062 Dresden, Germany
[b]Institut für Elektromechanische Konstruktionen, Technische Universität Darmstadt, 64283 Darmstadt, Germany

ABSTRACT

Dielectric elastomer actuators (DEAs) are compliant capacitors, which are able to transduce electrical into mechanical energy and vice versa. As they may be applied in different surrounding conditions and in applications with alternating excitations, it is necessary to investigate both, the thermal behavior and the influence of the temperature change during operation. Due to mechanical and electrical loss mechanisms during the energy transfer, the DEA is subjected to an intrinsic heating. In detail, the dielectric material, which has viscoelastic properties, shows a mechanical hysteresis under varying mechanical loads. This behavior leads to a viscoelastic loss of energy in the polymer layer, resulting in a heating of the structure. The non-ideal conduction of the electrode provokes a resistive loss when charging and discharging the electrode layer. Operation with frequencies in the kilohertz-range leads to remarkable local heat dissipation. The viscoelastic material behavior and the resistivity are assumed to be dependent on the temperature and/or on the strain of the material. By this, a back-coupling from the thermal field to the mechanical field or the electrical field is observed. In order to provide a thermal equilibrium, also the convective cooling – the structure is subjected to – has to be considered. Depending on the frequency and the type of electrical driving signal and mechanical load, viscoelastic and resistive heating provide different contributions during the dynamic process. In the present study we capture the described effects within our modeling approach. For a given dielectric elastomer actuator, numerical investigations are performed for a given electrical load.

Keywords: Dielectric Elastomers, Dynamic Loads, Power Loss, Numerical Simulation

1. INTRODUCTION

Dielectric elastomer actuators (DEAs) are smart structures, which are build as compliant capacitors. In these, the electrostatic attraction is used to deform an elastic dielectric structure. The working principle of DEAs is shown in Figure 1. An applied potential difference leads to a deformation of the depicted actuator. The application of DEAs with alternating excitations makes it necessary to consider the lossy process of energy conversion and the subsequentially heating of the structure. The observed temperature change for this kind of application has an influence on the material properties, which are decisive for the process itself. Therefore, a back-coupling from the thermal to the electromechanical field ensues. In 2016, Schlögl and Leyendecker have presented an electrostatic-viscoelastic finite element model of dielectric actuators.[1] In their work, a model for the static state is extended to capture the time dependent behavior of DEAs. Based on this, Mößinger et al.[2] presented a simulation model, in which the continous model approach of Schlögl et al. is combined with a complex lumped paremeter model by Haus et al.[3] The combined model is able to describe the transient behavior of DEAs. The occuring dissipation is considered in the work of Mößinger et al., but the development of the temperature field is not investigated. In the present paper a similar approach is used to simulate the thermal effects in dynamically driven DEAs. The purpose of the present work is to determine the resulting thermal field and the temperature change of the structure, due to lossy energy transformation.

Further author information: (Send correspondence to M. Kleo)
M. Kleo: E-mail: mario.kleo@tu-dresden.de

Electroactive Polymer Actuators and Devices (EAPAD) XX, edited by Yoseph Bar-Cohen,
Proc. of SPIE Vol. 10594, 105940G · © 2018 SPIE · CCC code:
0277-786X/18/$18 · doi: 10.1117/12.2295924

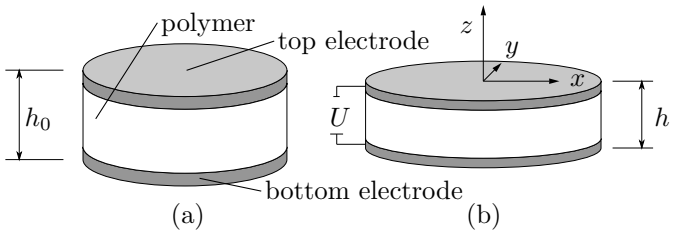

Figure 1. Dielectric elastomer actuator in the reference (a) and the deformed (b) configuration.

2. THEORY

In the present section, the thermo-electro-mechanical modeling of DEAs will be given. As the frequency of the applied electric field is low, the coupling to the magnetic field can be neglected and therefore it is not necessary to consider any influence of the magnetic field. Due to the slow processes, we will just use electrostatic formulations for the electric field. Additionally, the boundary effects are assumed to be insignificant due to the geometry of most of the DEAs, where the thickness of each layer is comparatively small in respect to the in-plane dimensions. In the electric field description, for the dielectric material, the constitutive relationship between the electric field $\vec{E}$ and the electric displacement $\vec{D}$ reads

$$\vec{D} = \epsilon \vec{E}\,, \tag{1}$$

where $\epsilon = \epsilon_0\,\epsilon_r$, is the absolute permittivity.

2.1 Electro-Mechanical Coupling

The CAUCHY stress $\mathbf{s}$ is defined as the sum of the MAXWELL stress $\mathbf{s}_{\text{Maxwell}}$ and the local mechanical stress $\mathbf{s}_{\text{Mechanical}}$ as in[4]

$$\mathbf{s} = \mathbf{s}_{\text{Maxwell}} + \mathbf{s}_{\text{Mechanical}}\,. \tag{2}$$

The electrical static and the mechanical field are coupled by the MAXWELL-stress tensor defined as[5]

$$\mathbf{s}_{\text{Maxwell}} = \epsilon \vec{E} \otimes \vec{E} - \frac{1}{2}\epsilon \vec{E}^2 \mathbf{I}\,, \tag{3}$$

The mechanical stress is formulated by the constitutive relation which can be described with strain energy function W. This leads to

$$\mathbf{s}_{\text{Mechanical}} = \rho \mathbf{F} \frac{\partial W}{\partial \mathbf{F}}\,. \tag{4}$$

where $\mathbf{F}$ is the deformation gradient tensor.

2.2 Dissipation in the Mechanical Field

The absorbtion of the mechanical energy per volume p_{mech} – the mechanical power – is defined as the product of stress $\mathbf{s}$ and the strain rate $\dot{\mathbf{e}}$.[6]

$$p_{\text{mech}} = \mathbf{s}\,\dot{\mathbf{e}}\,. \tag{5}$$

In a viscoelastic material, the mechanical power emerges from the elastic energy absorption rate p_{elast} and the viscous energy dissipation rate p_{visc}.

$$p_{\text{mech}} = p_{\text{elast}} + p_{\text{visc}}, \tag{6}$$

The **mechanical loss** of power per volume is equal to this viscous energy dissipation rate. Under a cyclic load, the area of the resulting hysteresis in the stress-strain curve is equal to the viscous power loss per volume and cycle. According to Figure 2, the mean value of the viscous power loss can be calculated by

$$\overline{p}_{\text{visc}} = u_{\text{cyc}}\, f_{\text{mech}}\,, \tag{7}$$

where u_{cyc} is the dissipated energy per volume and cycle and f_{mech} is the frequency of the mechanical excitation.

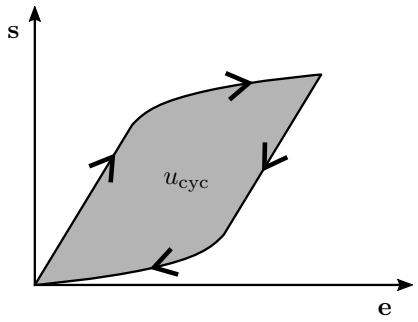

Figure 2. Schematic stress **s** versus strain **e** plot of a cyclic loaded viscous probe. The grey area of the hysteresis proportional to the dissipated energy per cycle u_{cyc}.

Due to the large deformations of the elastomer, we use hyper-viscoelastic material approach, including the OGDEN hyperelasticity.[7] The strain energy W is a function of the principal stretches λ_k and the material constants μ_i and α_i

$$W\left(\lambda_1, \lambda_2, \lambda_3\right) = \sum_{i=1}^{N=3} \frac{\mu_i}{\alpha_i} \left[\lambda_1^{\alpha_i} + \lambda_2^{\alpha_i} + \lambda_3^{\alpha_i} - 3\right] . \tag{8}$$

If the material constants are dependent on the time, they may be described with PRONY-series[8]

$$\mu_i(t) = \mu_{i,\infty} \left[\beta_\infty + \sum_{i=1}^{N=3} \beta_i \exp\left(-\frac{t}{\tau_i}\right)\right] \tag{9}$$

in order to get a viscous mechanical material behavior.

2.3 Dissipation in the Electrical Field

The volume density of the electric power p_{elec} can be calulated as the product of the electric current density $\vec{j}$ and the electric field strength $\vec{E}$

$$p_{\mathrm{elec}} = \vec{j} \cdot \vec{E} . \tag{10}$$

The electric current density is the sum of free $\vec{j}_{\mathrm{f}}$ and polarization $\vec{j}_{\mathrm{b}}$ current densities. They can be determined – according to balance of charge density $\mathfrak{q}$ – by

$$\vec{\nabla} \cdot \vec{j} = \vec{\nabla} \cdot \left(\vec{j}_{\mathrm{f}} + \vec{j}_{\mathrm{b}}\right) = -\frac{\partial \mathfrak{q}}{\partial t} = -\frac{\partial}{\partial t}\left(\mathfrak{q}_{\mathrm{f}} + \mathfrak{q}_{\mathrm{b}}\right) . \tag{11}$$

The non-ideal conductivity of the electrode leads to a **resistive loss**. The electrode is supposed to be a conductor, for which the free charge is dominant. In this case, Eq. (10) can be rewritten as:

$$p_{\mathrm{res}} = \vec{j}_{\mathrm{f}} \cdot \vec{E} . \tag{12}$$

By using the constitutive relation $\vec{j}_{\mathrm{f}} = \sigma \vec{E}$, where σ is the conductivity of the electrode, Eq. (12) can be given as

$$p_{\mathrm{res}} = \frac{1}{\sigma} \vec{j}_{\mathrm{f}}^{\,2} . \tag{13}$$

The conductivity is assumed to be potentially inhomogeneous as well as dependent on the temperature and the strain of the electrode, i.e. $\sigma = f\left(\vec{x}, T, \mathbf{e}\right)$.
To obtain the amount of the **dielectric loss** of power density, the dissipation occurring during the alignment of the dipoles within the electric field are considered. Since there is only charge bounded in the dielectric material, we can rewrite the previous formulation for the electric power with respect to the polarization current density $\vec{j}_{\mathrm{b}}$ by

$$p_{\mathrm{dielec}} = \vec{j}_{\mathrm{b}} \cdot \vec{E} . \tag{14}$$

The polarization current depends on the first order time derivative of the polarization field $\vec{j}_\mathrm{b} = \dfrac{\partial \vec{P}(t)}{\partial t}$ and thus on the material behavior of the dielectric medium.[9] If we assume a harmonic stimulus, we can determine the generated power density per volume by[10]

$$p_\mathrm{dielec} = \pi f \, \epsilon'' \, E_\mathrm{ampl}^2 \, . \tag{15}$$

Here, f represents the frequency of the harmonic excitation, ϵ'' is the imaginary part of the absolute permittivity and E_ampl is the amplitude of the harmonic electric field. Please note, that the material parameter ϵ'' itself is dependent on the frequency f.

2.4 Thermal Field

The total power loss, which occurs due to the dissipation in the electrical and mechanical energy transformation, is considered to be completely transfered into the volumetric heat source

$$q_\mathrm{total} = p_\mathrm{visc} + p_\mathrm{res} + p_\mathrm{dielec} \, . \tag{16}$$

The thermal field equation is formulated by:[11]

$$\rho \, \chi \, \frac{\partial T(\vec{x}, t)}{\partial t} + \vec{\nabla} \cdot \Big(\kappa \, \vec{\nabla} T(\vec{x}, t) + q_\mathrm{conv} \Big) = q_\mathrm{total}(\vec{x}, t) \, , \tag{17}$$

according to the different heat sources. In this equation T represents the temperature, ρ is the mass density, χ describes the specific heat capacity and κ stands for the thermal conductivity. The ambiance is considered by a surrounding matter (air) with constant temperature T_amb. The boundary condition of the probe is given as free convection

$$q_\mathrm{conv} = \alpha \, (T_\mathrm{surf} - T_\mathrm{amb}) \, , \tag{18}$$

where α is the heat transfer coefficient and T_surf the temperature of the respective sourface. In the case of DEA, three different zones of heat production can be distinguished. (I) Viscous and dielectric heating occurs in the active part of the polymer. (II) In the active part of the electrode, resistive and viscous heating is of interest. (III) In the the passive part of the electrode, only resistive heating takes place.

3. THERMO-ELECTRO-MECHANICAL SOLUTION PROCEDURE

The simulation of the thermal effects in the dynamically driven DEA is devided into two steps. In the first step, a coupled electromechanical simulation is performed and the result of the viscous, resistive and of the dielectric power loss is determined. In the following second step, the obtained power loss provides the thermal load for the subsequent thermal analysis. The solution procedure is illustrated in Figure 3.

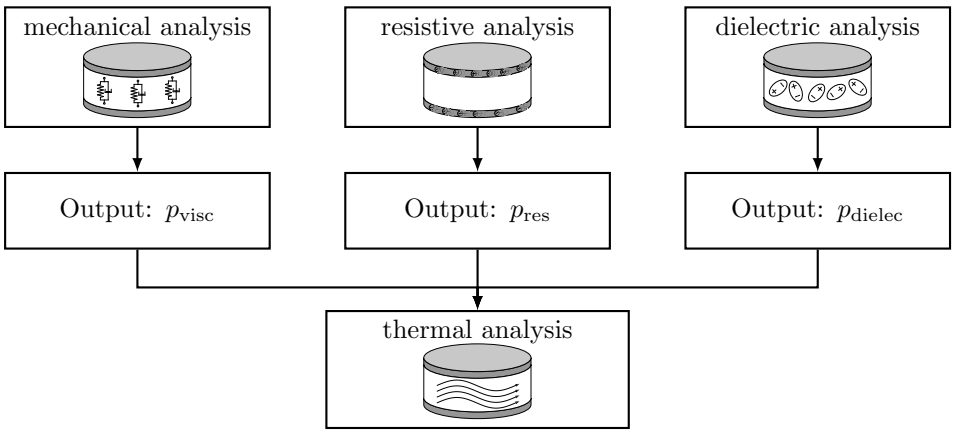

Figure 3. Illustration of the solution procedure

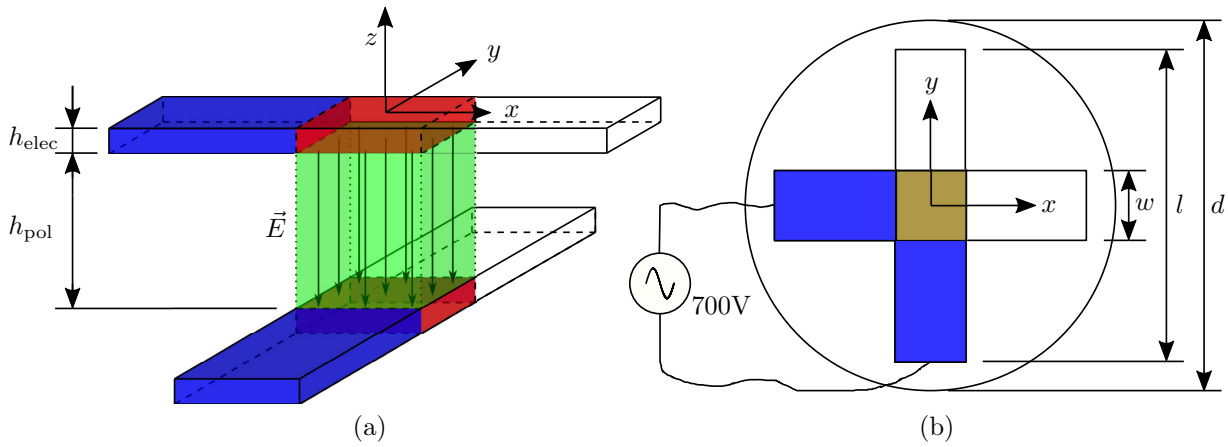

Figure 4. Schematic illustration of the geometric dimensions of the test-DEA. (a) alignment of the electrodes in the DEA, (b) DEA projected on the x-y plane. The heat production differs in the active part of the polymer (green), the active part of the electrode (red) and the passive part of the electrode (blue).

4. NUMERICAL SIMULATION

The investigated elastomer actuator has the geometric form of a stacked actuator with crosswise layered electrodes. The total number of polymer layers N is 50. It should be noted, that both, the top and bottom layer, are passive protective layers consisting of polymer. A schematic illustration of the test-DEA can be found in Figure 4. In between the overlaying parts of the electrode, the developing electric field in the intermediate dielectric material is supposed to be homogeneous. This region represents the active area of the actuation. The geometric dimensions of the test-DEA used in the numerical analysis are given in Table 1. According to the solution procedure, given in Figure 3, in the first step, the excitation is applied as a sinusoidal voltage load with an amplitude of 700 V and a frequency of 1 kHz. In the second step, an initial and ambient temperature of 20 °C is prescribed. Based on the difference in response time of the electromechanical and the thermal process, it is sufficient to apply the mean value of the power loss as a constant heat source over time and therefore neglect the alteration with the frequency f. The material parameters used in the simulation are given in Table 2. The numerical simulation is performed with the commercial finite elements tool ANSYS.

5. RESULTS

The cyclic loading of the structure leads to a power loss, resulting in a heating of the structure. In the first step, the electro-mechanical simulation, a mechanical stationary state is reached within a few seconds. In this state the viscous loss in the polymer is calculated. This viscous loss is distributed homogeneously in the volume of the active dielectric material. For the resistive loss, the change of the charge density in the electrode is calculated

Table 1. Geometric dimensions of the test-DEA used in the numerical simulation

Description	Symbol	Value
Geometry		
thickness of polymer layer	h_{pol}	$4.3 \cdot 10^{-5}$ m
thickness of electrode layer	h_{elec}	$7 \cdot 10^{-6}$ m
width of electrode	w	$5 \cdot 10^{-3}$ m
length of electrode	l	$3.5 \cdot 10^{-2}$ m
diameter of actuator	d	$4 \cdot 10^{-2}$ m
number of polymer layers	N	50

Table 2. Material parameters of the numerical simulation

Description	Symbol	Value
Mechanical material properties		
hyperelastic material parameter	μ_1	$6.3 \cdot 10^5 \frac{\mathrm{N}}{\mathrm{m}^2}$
hyperelastic material parameter	μ_2	$1.2 \cdot 10^3 \frac{\mathrm{N}}{\mathrm{m}^2}$
hyperelastic material parameter	μ_3	$-1 \cdot 10^4 \frac{\mathrm{N}}{\mathrm{m}^2}$
hyperelastic material parameter	α_1	1.3
hyperelastic material parameter	α_2	5
hyperelastic material parameter	α_3	-2
PRONY-series parameter	β_1	$1.3 \cdot 10^{-1}$
PRONY-series parameter	β_2	$7.5 \cdot 10^{-2}$
PRONY-series parameter	β_3	$3.3 \cdot 10^{-2}$
PRONY-series parameter	τ_1	$2.2 \cdot 10^{-2}\,\mathrm{s}$
PRONY-series parameter	τ_2	$4.0 \cdot 10^{-1}\,\mathrm{s}$
PRONY-series parameter	τ_3	$3.2 \cdot 10\,\mathrm{s}$
mass density	ρ	$1 \cdot 10^3 \frac{\mathrm{kg}}{\mathrm{m}^3}$
Electrodynamical material properties		
relative permittivity of polymer	ϵ_r	4.5
imaginary part of rel. perm. of polymer	ϵ_r''	$5 \cdot 10^{-4}$
electric conductivity of electrode	σ	$2 \cdot 10 \frac{\mathrm{S}}{\mathrm{m}}$
Thermodynamical material properties		
thermal conductivity of polymer	κ_{pol}	$2 \cdot 10^{-1} \frac{\mathrm{W}}{\mathrm{K \cdot m}}$
thermal conductivity of electrode	κ_{elec}	$1.2 \cdot 10^2 \frac{\mathrm{W}}{\mathrm{K \cdot m}}$
specific heat capacity of polymer	χ_{pol}	$1 \cdot 10^3 \frac{\mathrm{J}}{\mathrm{kg \cdot K}}$
specific heat capacity of electrode	χ_{elec}	$7 \cdot 10^2 \frac{\mathrm{J}}{\mathrm{kg \cdot K}}$
heat transfer coefficient	α	$2.5 \cdot 10 \frac{\mathrm{W}}{\mathrm{K \cdot m}^2}$

from the varying electric field. In Figure 5(a), the schematic electric current distribution in the electrode in space and time is shown. The resulting resistive heat density p_{res} applied to the active electrode has a quadratic form in x, see Figure 5(b). It is assumed to be constant in the width (y) and depth direction (z). The electric field also provides the input for the calculation of the dielectric loss. If the magnitudes of the examined heating sources are compared, it is clear, that the dielectric heating in the present example is negligible.

$$p_{\mathrm{visc}}, p_{\mathrm{res}} \gg p_{\mathrm{dielec}} \tag{19}$$

In Figure 6(a), a thermography of the test-DEA in equilibrium state is shown. As it can be seen in Figure 6(b) the numerical simulation of the thermal field establishes an equilibrium of the temperature at $t_{\mathrm{eq}} = 700\mathrm{s}$. Since the largest amount of heat is produced in the active parts of the electrodes, the highest temperature can be found here. Although the temperature is almost constant in thickness-direction, due to the small thickness of the layers. The quadratic distribution of the heat production in the electrode, with the highest value on the connected end and the lowest value on the free end, leads to the the peak of temperature at the area near to the voltage source.

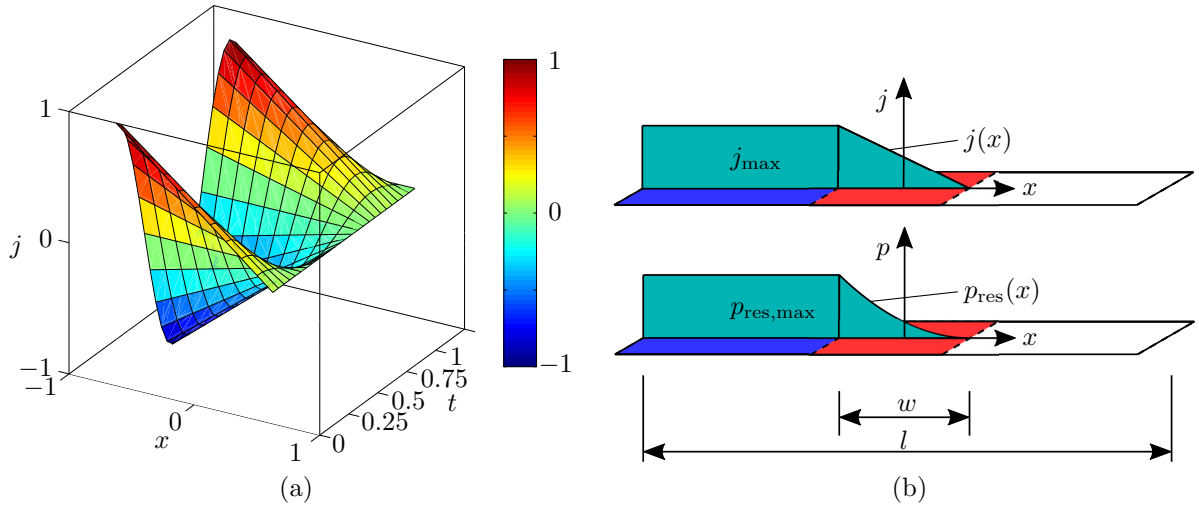

Figure 5. (a) Normalized loading current in the area of the overlaying electrodes resulting from an alternating excitation with a voltage at the boundary of $U(t) = U_0 \sin(2\pi f t)$. (b) Schematic profile of the amplitude of the loading current j (top) and schematic profile of the amplitude of the resistive heat source p_{res} (bottom), related to the location in the electrode.

6. CONCLUSION

In the present research, the mechanical and electrical loss mechanisms for a dielectric elastomer actuator (DEA) – under applied varying electric excitation – were investigated. The resulting significant heating of the structure can be simulated as consequence of the varying excitation. For this we have proposed a method, which is capable of determining the value of the heat source distribution coming from the energy dissipation of each process. In a subsequent analysis the development of the thermal field and thus of the temperature of the structure can be computed. However, governing material parameters may change during the transient process due to influences like temperature change. This behavior can be considered by an iteration, for which this work delivers the first cycle. To achive a more precise simulation, a full set of material parameters, in dependence of the temperature, is largely demanded.

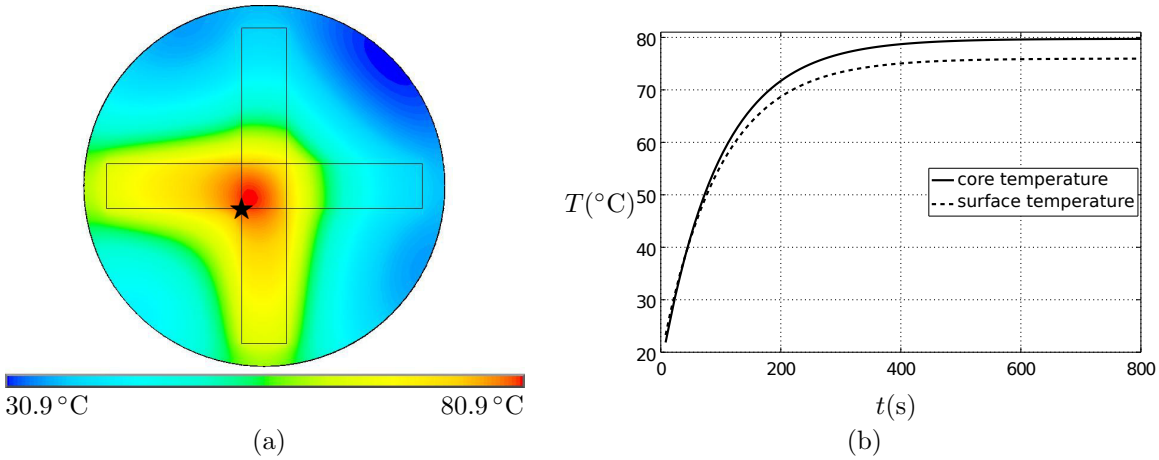

Figure 6. Results of the thermal analysis. (a) Thermography of the test-DEA in the equilibrium state in the middle layer (core), (b) Computed temperature development of a DEA of 50 layers at the location ★, regarding resistive and viscous heating and convective cooling.

REFERENCES

[1] Schlögl, T. and Leyendecker, S., "Electrostaticviscoelastic finite element model of dielectric actuators," *Computer Methods in Applied Mechanics and Engineering* **299**, 421 – 439 (2016).

[2] Mößinger, H., Förster-Zügel, F., and Schlaak, H. F., "Simulation of the transient electromechanical behaviour of dielectric elastomer transducers," *Proc. SPIE* **9798**, 979831–979831–10 (2016).

[3] Haus, H., Matysek, M., Mößinger, H., and Schlaak, H. F., "Modelling and characterization of dielectric elastomer stack actuators," *Smart Materials and Structures* **22**(10), 104009 (2013).

[4] Goulbourne, N., Mockensturm, E., and Frecker, M., "A Nonlinear Model for Dielectric Elastomer Membranes," *Journal of Applied Mechanics* **72**, 899–906 (November 2005).

[5] Eringen, A. C., [*Electrodynamics of continua - 1 : Foundations and solid media*], Springer, New York ; Heidelberg (1990).

[6] Tschoegl, N. W., [*The phenomenological theory of linear viscoelastic behavior: an introduction*], Springer Science & Business Media (2012).

[7] Ogden, R. W., "Large Deformation Isotropic Elasticity - On the Correlation of Theory and Experiment for Incompressible Rubberlike Solids," *Proceedings of the Royal Society of London. A. Mathematical and Physical Sciences* **326**(1567), 565–584 (1972).

[8] Brinson, H. F. and Brinson, L. C., [*Polymer engineering science and viscoelasticity / an introduction*], Springer, Springer (2008).

[9] Henke, H., [*Elektromagnetische Felder / Theorie und Anwendung*], Springer Berlin Heidelberg, Berlin, Heidelberg (2011).

[10] von Hippel, A. R., [*Dielectric and Waves*], Artech House (1995).

[11] Truesdell, C. and Toupin, R., [*The Classical Field Theories*], 226–858, Springer Berlin Heidelberg, Berlin, Heidelberg (1960).